

- between segmental mobility and the location of antigenic determinants in proteins. *Nature (Lond.)* 311:123–126.
3. Tainer, J. A., E. D. Getzoff, H. Alexander, R. A. Houghten, J. A. Olsen, R. A. Lerner, and W. A. Hendrickson. 1984. The reactivity of anti-peptide antibodies is a function of the atomic mobility of sites in a protein. *Nature (Lond.)* 312:127–134.
  4. Sheriff, S., W. A. Hendrickson, R. E. Stenkamp, L. C. Sieker, and L. J. Jensen. 1985. Influence of solvent accessibility and intermolecular contacts on atomic mobilities in hemerythrins. *Proc. Natl. Acad. Sci. USA* 82:1104–1107.
  5. Finzel, B. C., and F. R. Salemme. 1985. Lattice mobility and anomalous temperature factor behavior in cytochrome *c*'. *Nature (Lond.)* 315:686–688.

## MOTIONS OF TROPOMYOSIN

### Characterizations of Anisotropic Motions and Coupled Displacements in Crystals

DIMITRI BOYLAN AND GEORGE N. PHILLIPS, JR.

*Department of Physiology and Biophysics, University of Illinois, Urbana, Illinois 61801*

Tropomyosin is a 400-Å long  $\alpha$ -helical coiled-coil protein that winds around the actin filaments of muscle and, along with troponin, forms the regulatory “on-off” switch for muscle contraction. Two species of tropomyosin exist in skeletal muscle,  $\alpha$  and  $\beta$ , each comprised of 284 amino acids. In the crystal, tropomyosin molecules link end-to-end as they do in muscle, with an overlap of approximately eight or nine amino acid residues, to form long filaments that run parallel to body diagonals of the unit cell. These crystals are 95% solvent, and allow large-scale fluctuations of the filaments about their mean positions.

The crystal structure of tropomyosin has been solved to a resolution of  $\sim 15$  Å (1). Further analysis has revealed the average pitch and radius of the coiled-coil and the head-

to-tail overlap of adjacent molecules along the filament (2). Refinement of the structure using the method of least squares has yielded density profiles along the molecule that correlate with the amino acid sequence. Isotropic “temperature” factors that vary along the length of the molecule have also been determined.<sup>1</sup> The temperature factor function shows two minima in the fluctuations along each molecule, reflecting the steric hindrance from the cross-connection of molecular filaments in the lattice (Fig. 1).

Reversible temperature-sensitive changes in the COOH-terminal half of the molecule provide evidence that these

<sup>1</sup>Phillips, G. N., Jr., J. P. Fillers, and C. Cohen. Manuscript submitted for publication.

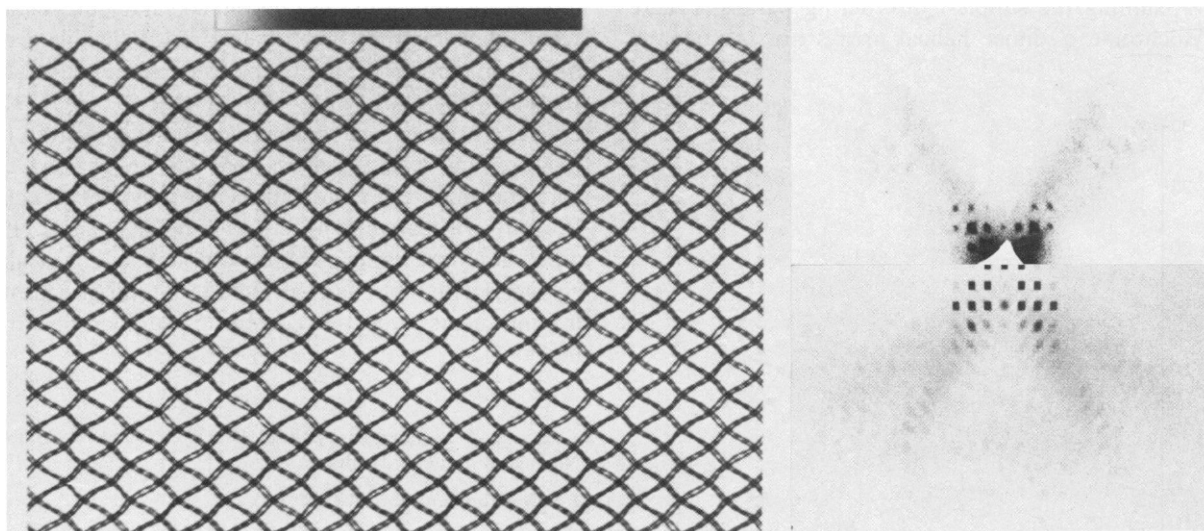


FIGURE 1 Comparison of observed and calculated diffuse x-ray scattering patterns. The simulated crystal lattice of tropomyosin is shown on the left. The function consists of an array of  $512 \times 512$  points, including 256 unit cells. The positions of the tropomyosin filaments are displaced from their average positions by including both random and wave-coupled perturbations. This array is Fourier-transformed, scaled, convoluted with a square to represent the x-ray beam size, corrected for the curvature of Ewald's sphere and displayed (lower right). The resulting theoretical pattern can be compared with the experimentally observed x-ray diffraction data (upper right). Aspects of the continuous scatter and the streaks near the Bragg peaks are accounted for by the simulation.

displacements are indeed "dynamic" rather than "static" in nature (2, 3). This temperature effect would not be expected in the case of lattice disorder (4). Further evidence for the motions of these filaments comes from estimates of the energy required to bend an  $\alpha$ -helical coiled-coil such as tropomyosin. Molecular bending forces can be estimated from theoretical considerations (5), or viscoelastic measurements (6). Either method yields values of  $\sim 130$  nm for the persistence length. The degree of bending of the molecular filaments in the crystal can be estimated from the rms fluctuations. The energy of the first-order bending modes of the molecules in the lattice is thus calculated to be 0.4–0.6 kT, approximately the amount of energy available from thermal motions of the surrounding water ( $\frac{1}{2}$  kT).

Here we report the extension of the crystallographic analysis to allow anisotropic "temperature" factors that vary along the length of the molecule. Resulting  $R$ -factors for the  $\alpha$  and  $\beta$  tropomyosin data sets are 0.18 and 0.12. Fig. 2 shows ellipses representing the thermal vibrations along two axes,  $v$  and  $w$ , perpendicular to the long axis of the molecule. The lengths of the principal axes are proportional to the rms displacements along these directions. In both the  $v$  and  $w$  directions there are minima whose locations correspond to regions where the molecules cross-connect in the lattice (see bars in Fig. 2). In general, displacements along the  $w$  axis are larger than those along the  $v$  axis. As in the isotropic refinement, the COOH-terminal half of the molecule shows greater flexibility than the NH<sub>2</sub>-terminal half. The largest anisotropy not found in the cross-connecting regions is found at the end-to-end overlaps region. These anisotropic motions seem to be

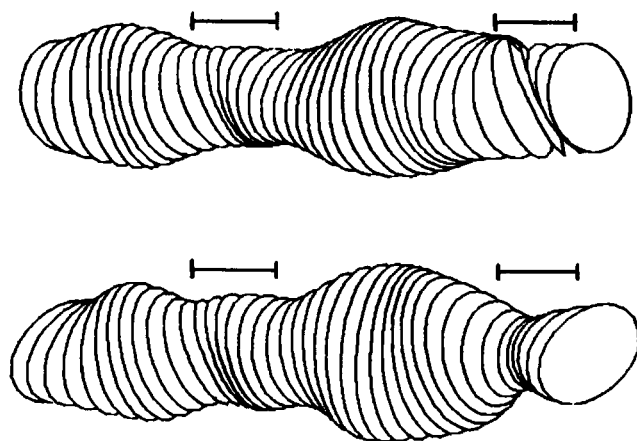


FIGURE 2 Probability ellipses representing the anisotropic temperature factors as a function of distance along the molecule for both  $\alpha$  form (bottom) and  $\beta$  forms (top) of tropomyosin. The varying lengths of the principal axes represent the rms displacements of the filaments from their mean positions. These ellipses have been scaled up by a factor of eight relative to the 50% probability ellipses to emphasize the anisotropic motions. Values for the rms displacements range from 0.3 Å at the cross-connecting regions to 8.9 Å in the COOH-terminal half of the molecule. Anisotropy is greatest at the cross-connecting regions (shown by bars) and at the ends of the molecule where overlap occurs.

consistent with the constraints imposed by the packing of the molecules in the lattice.

Motions of the filaments are also seen in other aspects of the diffraction pattern. Still photographs show strong streaks along certain directions (Fig. 1). The continuous diffuse scatter can be attributed to random displacements of the filaments from their average positions and can be analyzed to determine the basic units of collective motion and the magnitudes of their displacements. The fact that the streaks are not modulated by the lattice or unit cell packing transforms indicates that each arm of the lattice moves as a unit, with a high degree of randomness.

A certain degree of coupling of motions of molecules, however, would be expected to occur because of the lattice contacts. Excursions of the filaments from their average positions will produce a slight "pull" on the crossover regions. These forces would be expected to couple, to some degree, with the displacements in neighboring unit cells. It is difficult to quantify the force constants of this coupling, but we have accounted at least qualitatively for these effects. Generally speaking, the diffuse scattering near the Bragg peaks arises from coupled displacements between molecules (as opposed to the continuous diffuse scatter described in the previous section). If one defines a vector from the Bragg peak to a nearby point where diffuse scatter occurs, this same vector corresponds to a wave vector for propagations of displacements in the lattice. Each wave vector has one longitudinal and two transverse waves associated with it. The observed scattering of tropomyosin can be accounted for by simulating couplings of displacements along physically reasonable directions and calculating the diffraction patterns. The analysis reveals that waves of displacement are propagated along the directions of the molecular filaments.

We envision the mechanical properties of tropomyosin molecules in muscle to be similar to those in the crystal. The movement of tropomyosin from one state of regulation to the other requires a certain degree of flexibility, but yet it must be sufficiently stiff to provide cooperativity along actin during the activation process.

The method used here for analyzing the diffuse scatter from tropomyosin could be applied to other complex macromolecules to obtain information about their collective motions. One has to be able to predict that a few ( $\sim 20$  or less) states can adequately describe the range of conformations. Levitt et al. (8) have indeed shown that the rms fluctuations are usually dominated by a few slow modes. It should then be possible to test experimentally theories of protein normal-mode dynamics by studying diffuse scatter.

Received for publication 3 May 1985.

## REFERENCES

1. Phillips, G. N., Jr., E. E. Lattman, P. Cummins, K. Y. Lee, and C. Cohen. 1979. Crystal structure and molecular interactions of tropomyosin. *Nature (Lond.)* 278:413–417.

2. Phillips, G. N., Jr., J. P. Fillers, and C. Cohen. 1980. Motions of tropomyosin. *Biophys. J.* 32:485-502.
3. Phillips, G. N., Jr., and D. Boylan. 1984. Large scale fluctuations of tropomyosin in the crystal. *Trans. Amer. Cryst. Assoc.* 20:163-166.
4. Petsko, G. A., and D. Ringe. 1984. Fluctuations in protein structure form x-ray diffraction. *Annu. Rev. Biophys. Bioeng.* 13:331-371.
5. Suezaki, Y., and N. Gö. 1976. Fluctuations and mechanical strength of  $\alpha$ -helices of polyglycine and poly(L-alanine). *Biopolymers.* 15:2137-2153.
6. Hvidt, S., F. H. M. Nestler, M. L. Greaser, and J. D. Ferry. 1982. Flexibility of myosin rod determined from dilute solution viscoelastic measurements. *Biochemistry.* 21:4064-4073.
7. Levitt, M., C. Sander, and P. S. Stern. 1985. Protein normal-mode dynamics: trypsin inhibitor, crambin, ribonuclease and lysozyme. *J. Mol. Biol.* 181:423-447.

## DETERMINANTS OF COLLAGEN FIBRIL STRUCTURE

BARBARA BRODSKY AND ERIC F. EIKENBERRY

*Departments of Biochemistry and Pathology, University of Medicine and Dentistry of New Jersey, Rutgers Medical School, Piscataway, New Jersey 08854*

The group of tissues that are classified as connective tissues all contain collagen as a major structural protein that is characteristically found in the form of long, cylindrical fibrils with an axial period of  $D = 67$  nm. Within this group, different connective tissues, such as tendon, bone, cartilage, and skin, show distinct physical and mechanical properties that appear to be related to the presence of specific genetic types of collagen. For example, the collagen of tendon and of bone is almost exclusively type I collagen, the most common of the several different genetic types. Cartilage, notochord, and the vitreous body of the eye contain largely type II collagen. Other tissues contain specific mixtures of different genetic types; for example, skin contains type I collagen mixed with 15-20% of type III.

The tissue-specific properties are accompanied by variations in the lateral structure of collagen fibrils. Variations among different tissue types include differences in the diameter of fibrils, which range from 8 to 600 nm; the distribution of fibril diameters, which vary from monodisperse to highly polydisperse; and the packing of fibrils, which may be tightly or loosely packed. Variations continue at the molecular level where the lateral organization of molecules ranges from crystalline to highly disordered. The range of variation in lateral molecular packing and fibril architecture is being characterized using x-ray fiber diffraction and electron microscopy. Such characterizations are a first step in understanding the interactions and forces that create and stabilize the tissue-specific structures that are observed.

Rat tail tendon (RTT) is the tissue in which the fibril structure is known in most detail. RTT gives excellent x-ray diffraction patterns because the fibrils are well oriented and contain type I collagen molecules organized in large crystalline domains. The discrete Bragg reflections that sample the equatorial molecular transform and the first layer line of the triple-helical pitch at  $1/9.5$  nm<sup>-1</sup> have made it possible to define precisely the three-dimensional unit cell of RTT, the orientation of the cell with respect to

the fibril axis and the location of the molecules within the cell (1, 2). In addition to the discrete reflections, there is a diffuse background along the equator, indicating that part of the molecules are in a state less ordered than crystalline. Recent analysis by Fraser, et al. (3) has suggested that along each fibril there is an alternation between crystalline domains comprising 0.47 of each  $D$  repeating unit (the overlap region) and disordered domains comprising 0.53  $D$  (the gap region).

The notochord sheath of the lamprey, which contains type II collagen, has recently been shown to have well-oriented collagen fibrils of very small diameter (17 nm) in which the collagen molecules are packed in crystalline arrays (4). The axial period is the same as RTT (67 nm) but the lateral structure is considerably different. The unit cell proposed for the lamprey notochord collagen structure is 40% larger in volume than that of RTT, an increase which is largely the result of lengthening of one cell edge. The increase in volume may be caused by the considerably increased level of glycosylation and attendant hydration that type II collagen exhibits in comparison to type I. These specimens also show diffuse scatter along the equator, suggesting the presence of disordered portions of the structure as in RTT. The profile of this scatter indicates that, in comparison to type I, there is a lower density of collagen molecules in the disordered domains of type II as well as in the crystalline regions.

Most tissues, other than RTT and lamprey notochord sheath, do not show crystalline Bragg reflections sampling the molecular transform on the equator; instead they give only diffuse equatorial scattering, indicative of a laterally disordered structure. The scattering is in the form of a single broad maximum which, for most tendons, demineralized bones, and skins, is located at various spacings ranging from  $1/1.47$  nm<sup>-1</sup> to  $1/1.58$  nm<sup>-1</sup> (5). The breadth of the maximum varies from one tissue to another. Such a maximum represents the product of the molecular transform and the interference function arising from the lateral spatial correlation of the molecular positions. Divi-